

Limitation of the electron emission in an ion diode with magnetic self-insulation

A. I. Pushkarev, Yu. I. Isakova, and V. I. Guselnikov
Tomsk Polytechnic University, 30, Lenin Ave., Tomsk 634050, Russia

(Received 11 May 2011; accepted 26 July 2011; published online 25 August 2011)

The results of a study of the generation of a pulsed ion beam of gigawatt power formed by a diode with an explosive-emission potential electrode in a mode of magnetic self-insulation are presented. The studies were conducted at the TEMP-4M ion accelerator set in double pulse formation mode: the first pulse was negative (300–500 ns and 100–150 kV) and the second, positive (150 ns and 250–300 kV). The ion current density was 20–40 A/cm²; the beam composition was protons and carbon ions. It was shown that plasma is effectively formed over the entire working surface of the graphite potential electrode. During the ion beam generation, a condition of magnetic cutoff of electrons along the entire length of the diode ($B/B_{cr} \geq 4$) is fulfilled. Because of the high drift rate, the residence time of the electrons and protons in the anode–cathode gap is 3–5 ns, while for the C⁺ carbon ions, it is more than 8 ns. This denotes low efficiency of magnetic self-insulation in a diode of such a design. At the same time, it has been experimentally observed that, during the generation of ion current (second pulse), the electronic component of the total current is suppressed by a factor of 1.5–2 for a strip diode with plane and focusing geometry. A new model of the effect of limiting the electron emission explaining the decrease in the electronic component of the total current in a diode with magnetic self-insulation is proposed. © 2011 American Institute of Physics. [doi:10.1063/1.3626555]

I. INTRODUCTION

Planar diodes, with explosive-emission cathodes, are widely used for the generation of wide-aperture pulsed ion and electron beams with a current density of more than 20 A/cm². Studies have shown that, after application of voltage to the diode and the formation of anode plasma, the generation of electron and ion currents occurs simultaneously, and the current density is limited by the space charge.¹ The current density of protons (in the mode of space charge limitation) is 2.3% of the electron current density. The density of a heavier ion is lower. For effective generation of ion beams, it is necessary to ensure the suppression of the electronic component of the total diode current. In 1973, Sudan and Lovelace² first suggested constructing a pulsed ion diode with external magnetic insulation. The magnetic field causes the electron trajectory to bend (under the Lorentz force) by 90° ($B > B_{critical}$) as the electrons drift across the electric field in the anode–cathode (A-K) gap.³ However, an additional energy source for the formation of the magnetic field increases the power consumption of the generator. For a total ion beam energy of 80–90 J per pulse, up to 500 J is required from the magnetic field source.⁴ In 1977, Humphries⁵ first suggested the construction of an ion diode with magnetic self-insulation. A transverse magnetic field is formed in the A-K gap by the diode self-current when the current flows along the electrodes. In this case, an additional magnetic field source is not required. This significantly simplifies the construction of the pulsed ion beam generator. But the efficiency of ion current generation in diodes with magnetic self-insulation does not exceed 5%–10%,⁶ which limits their application.

In spite of much progress in the development of powerful ion beam (PIB) sources, many processes in an ion diode with magnetic self-insulation have not been researched enough. In particular, no analysis of the mechanism of suppression of the electron current has been performed, nor have the reasons for the low efficiency of the PIB generation been discovered. This can be explained in the following way: during the first 25–30 years, the main application of pulsed ion beams was in controlled thermonuclear fusion investigations. The production of ion beams with maximum current density and a pulse power of more than 10¹² W was mostly attempted.

The first results of a systematic investigation of explosive emission plasma dynamics and ion current density in a diode with magnetic self-insulation were reported by Zhu *et al.*⁷ But the authors did not analyze the efficiency of magnetic self-insulation. A detailed review of studies on diodes with magnetic self-insulation is given in a monograph of V. Bystrickii⁶ and our papers.^{8,9} The purpose of this research is to investigate the electron current suppression in the ion diode with magnetic self-insulation.

II. EXPERIMENTAL SET-UP AND CALCULATIONS

Investigations were conducted at the TEMP-4M accelerator¹⁰ set in a double pulse mode: the first pulse is negative (300–500 ns and 100–150 kV) and the second is positive (150 ns and 200–250 kV). The beam composition is ions of carbon, C⁺, and protons; the ion current density is 20–150 A/cm² (for different types of diodes); and the pulse frequency is 5–10 pulses per minute. The accelerator consists of a capacitive storage-generator of pulsed voltage (the Marx

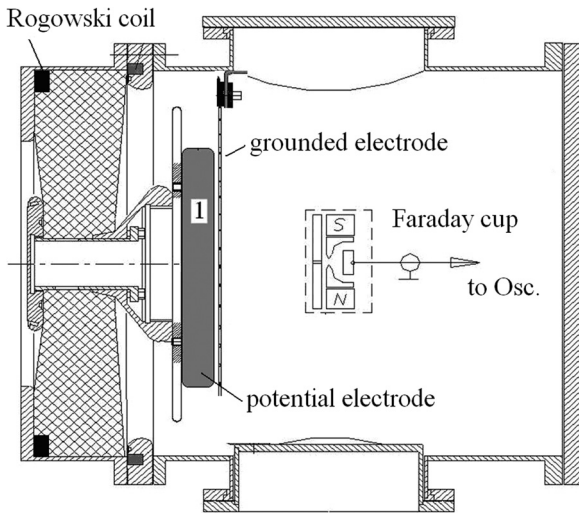


FIG. 1. Diode connection of TEMP-4M accelerator.

generator), a nanosecond double forming line (the Blumlein line), and a vacuum ion diode with magnetic self-insulation of the electrons. In the diode with magnetic self-insulation, the transverse magnetic field in the A-K gap is formed by the diode's self-current while it flows on a strip electrode. For this purpose, it is grounded at one point only. We studied the strip diode (22 cm \times 4.5 cm with a gap of 8–9 mm) with a potential graphite electrode. Figure 1 shows a scheme of the diode connection in the TEMP-4M accelerator and the voltage and current measurement. To measure the total current consumed by the diode connection, a Rogowski coil with a reverse loop was used. The ion current density was measured by a collimated Faraday cup with a magnetic cutoff of the electrons (0.4 T). The voltage on the potential electrode was measured by a high-frequency high-voltage divider which was installed in front of the diode connection. The electrical signals coming from sensors were recorded with a Tektronix 3052B oscilloscope (500 MHz, 5×10^9 measurements per second).

The inaccuracy of electrical signal synchronization did not exceed 0.5 ns. Figure 2 displays the waveforms of the

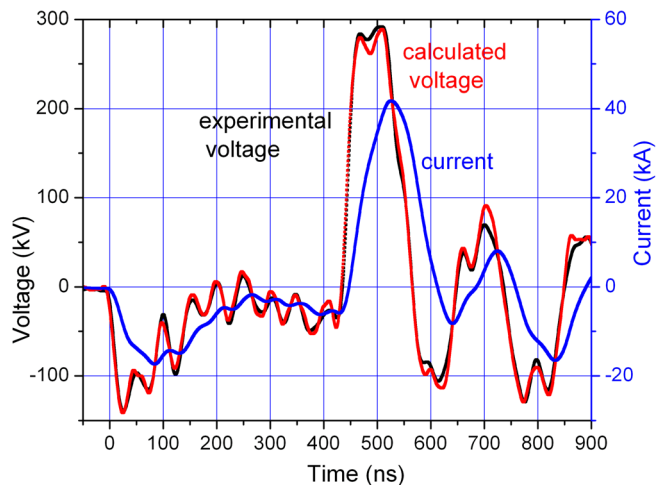


FIG. 2. (Color online) Waveforms of the total current and voltage on the potential electrode.

total current and accelerating voltage (experimental and calculated values).

These results were obtained using a 5.2 Ohm resistor during calibration. Calculation of the voltage was performed using the relation $U_{\text{calc}}(t) = R_{\text{load}} \cdot I(t) + L_{\text{load}} \cdot dI/dt$, where L_{load} is parasitic load inductance, 240 nH. Calculation of the inductance was made from the ratio for a straight conductor at a frequency of 1–10 MHz.¹¹ The calibration of the diagnostic equipment showed that it correctly reflected the accelerator operation in short circuit mode ($U = 50$ –60 kV) and when operating with a resistive load of up to 10 Ω (200–250 kV). The accuracy of the measurement of voltage and the total diode current as well as the frequency characteristics of the diagnostic equipment allows us to calculate the ion and electron current with an accuracy better than 10%.

Figure 3 shows typical waveforms which characterize the operation of the planar diode in the mode of magnetic self-insulation. Figure 3 also shows the calculated values of both electron and ion currents in the mode of space charge limitation.

Calibration of the diode's diagnostics (see Fig. 2) was performed using a resistive load, which has a parasitic inductance of 240 nH. The actual ion diode is smaller and its inductance does not exceed 50–80 nH, therefore, the voltage pulse applied to the diode (see Fig. 3) has a more sharp form.

When both the electron and ion currents density are more than 20 A/cm², the total current is limited by the space charge.¹ Taking into account the reduction in the A-K gap spacing due to the plasma emitting surface expansion,^{8,9} the electron current is equal to

$$I_e(t) = \frac{4\epsilon_0\sqrt{2e}}{9\sqrt{m_e}} \cdot \frac{U^{3/2} \cdot S}{d^2} = \frac{2.33 \cdot 10^{-6} \cdot U^{3/2} \cdot S}{(d_0 - vt)^2}, \quad (1)$$

where U is the voltage applied to the diode, d_0 is the initial A-K gap, m_e is the electron mass, e is the electron charge, S is the area of the potential electrode, and v is the plasma expansion rate.

When the applied voltage polarity reverses the bipolar flow in the A-K is established. Ions start from the potential electrode (graphite) and move into the A-K gap towards the

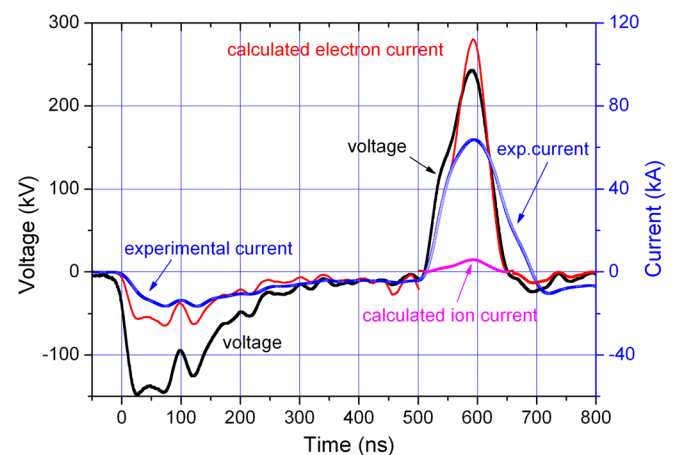


FIG. 3. (Color online) Waveforms of accelerating voltage, total current in the planar diode, and calculated currents of electrons and ions. Gap is 8 mm.

grounded electrode. These ions are removed from the graphite plasma front surface causing the thinning of plasma layer which leads to an increase in the effective vacuum gap spacing. In this case when calculating the ion current, it is necessary to consider not only the reduction in the A-K gap due to plasma heat expansion as in the relation (1) but also the increasing of the effective gap spacing due the plasma erosion¹² when the polarity on the potential electrode changes. This is taken into account in the dominator of relation (2) by subtracting from the current time t the time t_0 . By doing that, we create the condition when the A-K gap spacing is not filled with plasma as at the beginning of the first voltage pulse ($t = 0$ in Fig. 2).

$$I_{ion}(t) = \frac{4\epsilon_0\sqrt{2z}}{9\sqrt{m_i}} \cdot \frac{U^{3/2} \cdot S}{[d_0 - v \cdot (t - t_0)]^2}, \quad (2)$$

where m_i and z are the ion mass and charge, respectively, and t_0 is the time of arrival of the second pulse ($t_0 = 500$ ns in Fig. 3).

In the Eqs. (1) and (2), t is the current time of voltage. The moment $t = 0$ corresponds to the 0.1 level of the amplitude of the first (negative) pulse.

The studies¹³ show that, from the application of the voltage until a continuous plasma surface is formed on the potential electrode (the mode of discrete emitting surface, $0 < t < 200$ ns in Fig. 3), the diode current is limited by the emissivity of the cathode and is lower than the calculated Child-Langmuir (CL) value. After the potential electrode surface is covered by plasma (200 ns $< t < 500$ ns), the total diode current is limited only by the space charge of electrons in the A-K gap. Experimental values of the total current are satisfactorily described by the CL value obtained from Eq. (1) at a constant rate of plasma expansion equal to 1.3 cm/ μ s. The operation of the ion diode in this case is similar to an electron diode with an explosive emission cathode.¹⁴ During the PIB generation (second pulse), suppression of the electronic component of the total current by a factor of 1.5–2 occurs for the strip diode with plane and focusing geometry. But, because the ion component does not exceed 10% of the total diode current (see Fig. 3), technical applications of the diodes with magnetic self-insulation are limited.

III. ANALYSIS OF THE CHANGE IN MAGNETIC INSULATION OVER THE LENGTH OF THE DIODE

On the first pulse, the electrons start from the potential electrode and move into the A-K gap towards the grounded electrode, which is connected to the housing of the diode chamber on one side only. Further, the electrons move along the electrode to the grounding point, forming a magnetic field in the gap. Therefore, subsequent electrons moving across the A-K gap arrive at the magnetic field and change trajectory. When the magnetic induction reaches a critical value B_{cr} , the electrons drift along the A-K gap. During the PIB generation, the electrons are emitted from the surface of the grounded electrode and then drift along its surface from the grounding point to the free end of the electrode. A sketch of the electrons' motion on the second pulse is shown in Fig. 4.

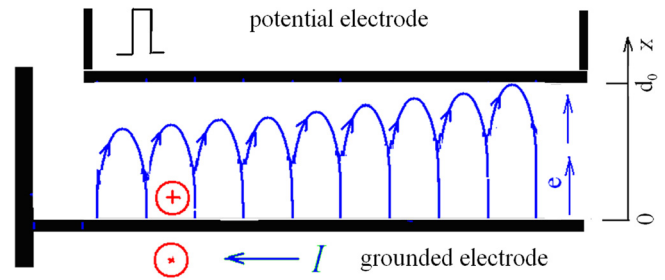


FIG. 4. (Color online) Scheme of the electrons' motion in the diode on the second pulse.

A possible reason for the low efficiency of suppression of the electron current in the diode with magnetic self-insulation is a low-induction magnetic field ($B < B_{cr}$) at the end of the diode. The electrons which are emitted from the grounded electrode surface immediately reach the potential electrode (see Fig. 4), reducing the efficiency of magnetic insulation.

In the mode when current is limited by the space charge, the current density of singly ionized carbon ions is 0.7% of the electron current density (see Eqs. (1) and (2)). The optimization of both the design of the TEMP-4M accelerator and the operation mode of the ion diode with magnetic insulation resulted in an increase in the efficiency of ion current generation by a factor of 10–12.⁸ However, the ion component does not exceed 10% of the total diode current (see Fig. 3). Taking into account the increase in the effective vacuum gap spacing⁹ (after the applied voltage polarity changes) and a subsequent reduction due to expansion of the plasma, the area of the non-magnetized region of the diode $S_{nm}(t)$ can be calculated as a ratio of total current $I(t)$ to electron current density $J_e(t)$ at the space charge limitation

$$S(t) = \frac{I(t)}{J_e(t)} = \frac{I(t) \cdot [d_0 - v \cdot (t - t_0)]^2}{2.33 \cdot 10^{-6} \cdot 1.86 \cdot U^{3/2}},$$

where $J_e(t)$ is the electron current density in the mode of space charge limitation.

During the ion current generation, the space charge of electrons near the surface of the grounded electrode (which is the cathode on the second pulse) is partly compensated by ions from the potential electrode. In the A-K gap, the bipolar flow is realized and as a result, the electron current density increases by a factor of 1.86.¹⁵ It is taken into account, when calculating the area of non-magnetized surface. The results are shown in Fig. 5.

Within 40–50 ns after the reversal of voltage polarity ($510 < t < 550$ ns in Fig. 5), magnetic insulation of the electrons is negligible and the area of the non-magnetized part of the diode equals its total area. As the total diode current increases, a decrease in the emitting surface is observed, which may be associated with a magnetic cut-off of part of the diode. If the total current in the diode with magnetic self-insulation is determined by the area of the non-magnetized region of the diode, this area should exceed 50% of the total area. In this region, the value of magnetic induction should be less than the critical magnetic induction.

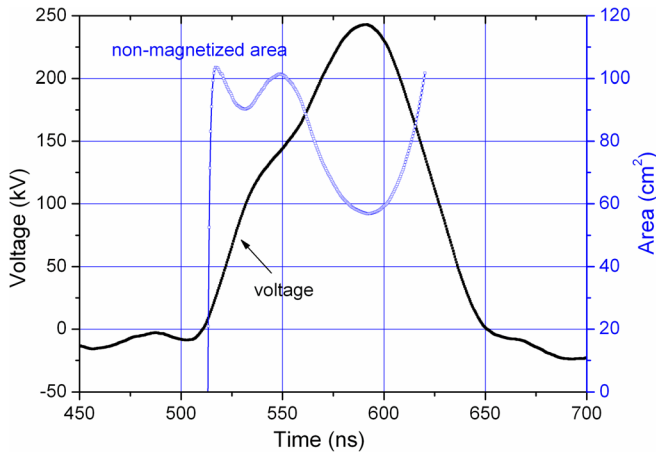


FIG. 5. (Color online) Change in the accelerating voltage and area of non-magnetized emission surface of the grounded electrode. Gap of 8 mm; and the geometric area of the diode is 100 cm².

The area of the non-magnetized part of the diode can be also estimated by comparing the magnetic induction in the A-K gap with the critical magnetic induction. In the calculation of the critical magnetic induction in the diode with an explosive potential electrode on the second pulse, both the reduction in the A-K gap (due to plasma expansion) and the increasing of the effective gap spacing in the A-K gap (due to plasma erosion) should be taken into account. Then

$$B_{cr1} = \frac{1}{d(t)} \sqrt{\frac{2m_e \cdot U(t)}{e}} = \frac{3.37 \cdot 10^{-6} \sqrt{U}}{d_0 - vt}; \quad \text{and}$$

$$B_{cr2} = \frac{3.37 \cdot 10^{-6} \sqrt{U}}{d_0 - v \cdot (t - t_0)},$$

where B_{cr1} and B_{cr2} are the critical magnetic induction on the first and second pulses.

The distribution of magnetic induction in the A-K gap was performed by the Elcut program. Figure 6 shows the distribution of the induction in the cross section of the diode.

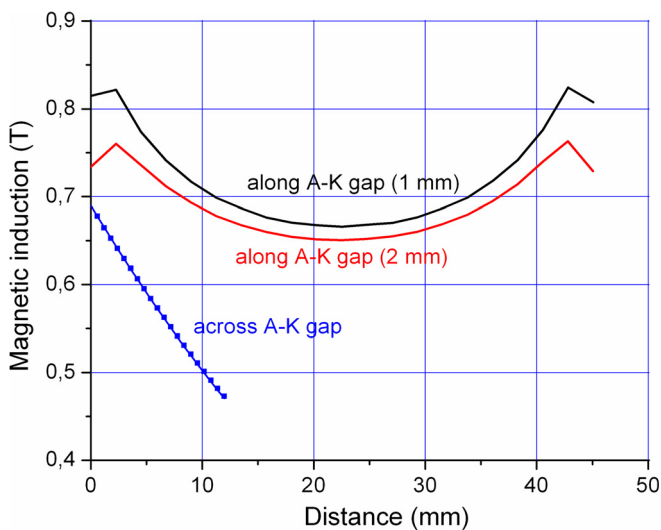


FIG. 6. (Color online) The distribution of magnetic induction in the cross section of the diode along the surface of the grounded electrode at distances of 1 mm and 2 mm and across the A-K gap in the center of the diode.

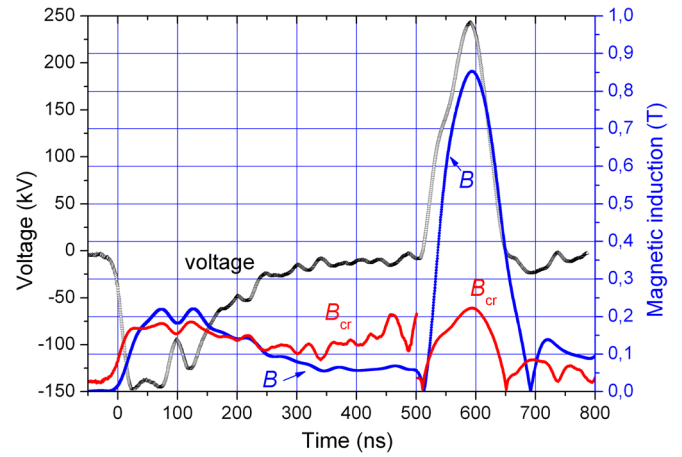


FIG. 7. (Color online) Waveform of accelerating voltage, critical magnetic induction B_{cr} , and magnetic induction B .

The calculation was performed at a current of 50 kA without considering the damping of the alternating magnetic field by the material of the potential electrode. The surface of the grounded electrode corresponds to distance $x = 0$ (curve “across A-K gap” in Fig. 6) in the first and second pulses. Figure 7 shows the change in induction of the magnetic field in the A-K gap of the diode with magnetic self-insulation and the change in the critical magnetic induction.

The calculation was performed for a region located at a distance of 0.5 mm from the surface of the grounded electrode for the total current on the grounded electrode. In our conditions during the ion beam generation, the magnetic induction in the A-K gap exceeds the critical induction by a factor of 4. Therefore, if the electron emission occurs uniformly over the length of the diode and the electrons which drift in the A-K gap do not contribute to the formation of a magnetic field then the area of the non-magnetized region of the diode does not exceed 20%–25%. The magnetic induction in the electron drift region (for the diode with magnetic self-insulation) is comparable with the magnetic induction in a diode with an external magnetic insulation, where an efficiency of ion current generation of over 80% of the total current was achieved.⁴

Figure 8 shows the results of a study of homogeneity of the electron beam generation in a flat diode. The distribution of energy density was measured by means of a thermal imaging technique¹⁶ adapted to the double-pulse mode. Experimental studies have shown that, in the diode with magnetic self-insulation, the plasma forms effectively on the entire working surface of the potential electrode and the PIB generation is fairly homogeneous.

To assess the contribution of the electrons drifting in the A-K gap to the formation of the magnetic field, it is necessary to calculate the thickness of the layer of their movement. The height of the trochoid of the electron drift motion¹² in the diode with magnetic insulation on the second pulse is equal to

$$\Delta_2(t) = \frac{2m_e \cdot E}{e \cdot B^2} = \frac{2m_e \cdot U(t)}{e[d_0 - v \cdot (t - t_0)]B(x, t)^2}.$$

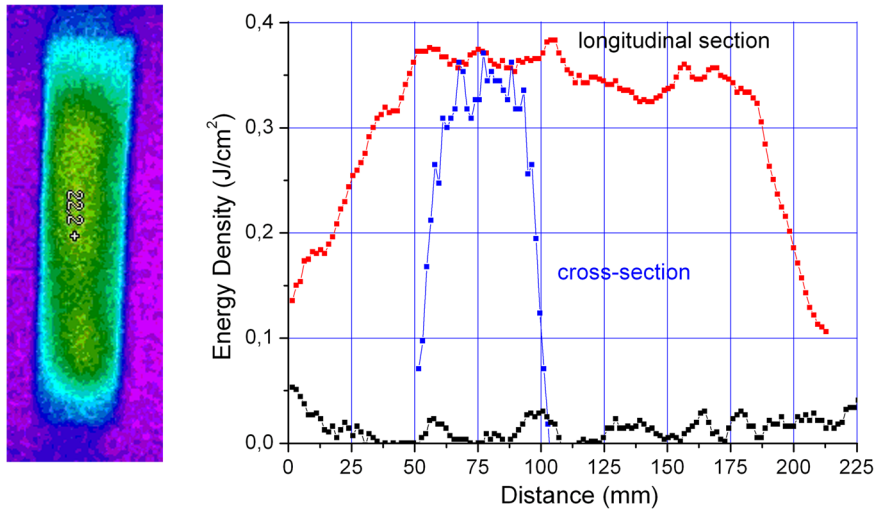


FIG. 8. (Color online) Thermal imprint and the energy density distribution on a brass target with thickness of $80 \mu\text{m}$. The distance from the diode to the target is 5 cm.

Figure 9 shows a change in the height of the trochoid of the electron drift motion at the generation of the ion beam.

The calculation was performed assuming that the magnetic induction in the gap is constant and equals the magnetic induction at a distance of 1 mm from the grounded electrode. The height of the trochoid of the electron drift motion (during the generation of ions in the diode with magnetic self-insulation) is comparable with the height of the layer of the electrons' drift in the diode with an external magnetic insulation, where a high efficiency of the PIB generation was achieved.⁴

In our experimental conditions, the thickness of the drifting electrons is less than 0.5 mm. The thickness of a skin layer in the grounded electrode, which is made from stainless steel, is 0.12 mm for the current frequency of 2.5 MHz (the current pulse duration is 200 ns, see Fig. 3). Then, the magnetic induction in the working part of the A-K gap equals the sum of the magnetic induction of the current flowing through the grounded electrode and the magnetic induction of the electrons which drift along its surface. The electrons in the skin layer and the drift region move in one direction (see Fig. 4) and, therefore, along the entire strip diode, the induction of magnetic field in the A-K gap significantly exceeds the critical induction.

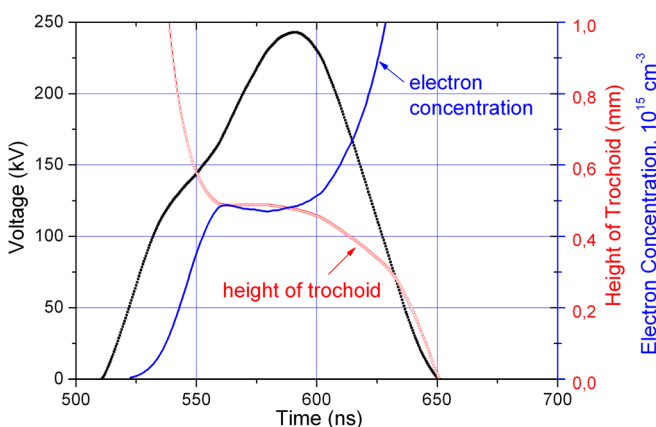


FIG. 9. (Color online) Oscilloscope traces of accelerating voltage, change in height of the trochoid of the electrons' drift motion, and the electron concentration in the drift region.

Provided that the total diode current equals the current of the drifting electrons (the ion current is small and the electrons do not leave the drift region), the concentration of the drifting electrons n_{dr} can be calculated from

$$n_{dr}(t) = \frac{I(t)}{S_{dr} \cdot e \cdot v_{dr}(t)} = \frac{I(t)}{e \cdot h \cdot \Delta(t) \cdot v_{dr}(t)},$$

where S_{dr} is the drift region section and h is the width of the electrode.

The concentration of the drifting electrons varies along the length of the diode from 0 (at the grounding point) to a value determined by the rate of drift, the total current, and the thickness of the drift region. Figure 9 shows a change in the concentration of electrons in the drift region near the free end (not grounded side of the diode) of the diode.

The analysis shows that, if the total current in the diode with magnetic self-insulation is determined by the area of the non-magnetized region of the diode, then this area should exceed 50% of the total area of the diode (see Fig. 5). But this area does not exceed 25% of the planar diode even without considering the contribution of the drifting electrons. Therefore, the low efficiency of the electron current suppression in the diode with magnetic self-insulation cannot be due to the region with a low magnetic field induction at the bottom of the diode.

The correctness of our calculations was confirmed by an experimental study of the formation of an additional transverse magnetic field in the gap using permanent magnets (0.1–0.15 T, placed opposite and parallel to the magnetic field of self-insulation) and with the current flowing on the strip grounded electrode from an external source (5–7 kA, a different polarity). The value of the total diode current in this case did not differ from data obtained without the formation of the additional magnetic field in the gap.

IV. CALCULATION OF THE ELECTRON DRIFT TIME

The effectiveness of the electronic component suppression in diodes with magnetic self-insulation is determined by the residence time of the electrons and ions in the A-K gap. If during the whole accelerating voltage pulse the electrons

drift along the electrode surface of the diode (perpendicular to the electric field lines) then, the energy of a nanosecond generator will be mainly used to accelerate the ions. But at a high drift rate of the magnetized electrons, the efficiency of suppression of the electron current is low.

On the first pulse, the electrons start from the potential electrode and move across the A-K gap to the grounded electrode, which is connected to the housing on one side only. Next, the electrons move along the electrode towards the grounding point, forming a magnetic field in the gap. Therefore, as they move across the gap, the electrons go into a stronger magnetic field and change their direction. When the induction of the magnetic field reaches a critical value B_{cr} , the electrons begin to drift along the A-K gap. Then, for the first pulse, the electrons' drift speed is

$$v_{dr1}(t) = \frac{E}{B} = \frac{U}{d \cdot B_{cr}} = \sqrt{\frac{e \cdot U}{2m_e}}$$

In calculating the electrons' drift velocity on the second pulse, it is necessary to consider the reduction in the A-K gap and the increase in the effective gap spacing when the polarity of the accelerating voltage reverses

$$v_{dr2}(t) = \frac{U(t)}{[d_0 - v(t - t_0)]B(t)}.$$

For the second pulse, the calculation was carried out on the assumption of a constant magnetic induction in the gap which equals the magnetic induction at a distance of 0.5 mm from the grounded electrode. Figure 10 shows the change in the electrons' drift velocity in the A-K gap.

The optimization of the operation of the diode with magnetic self-insulation resulted in reduction of the electrons' drift velocity to 30–40 mm/ns, which is 2 times lower than the drift velocity of the electrons in the diode with the external magnetic field.⁴

Under the condition that the ions in the A-K gap are uniformly accelerated, the duration of their acceleration is

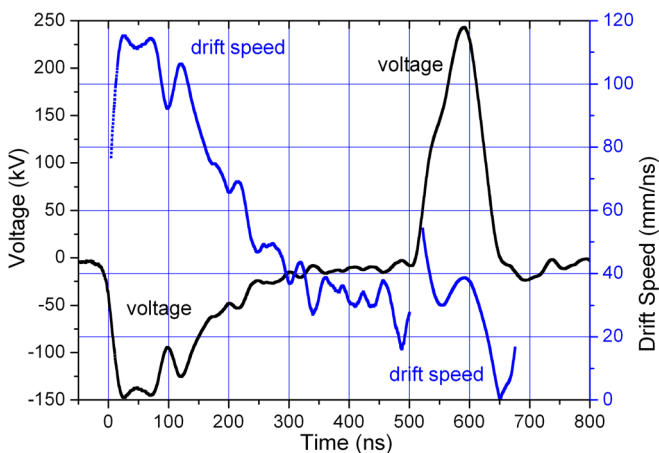


FIG. 10. (Color online) Oscilloscope trace of the accelerating voltage and the change in the electrons' drift velocity.

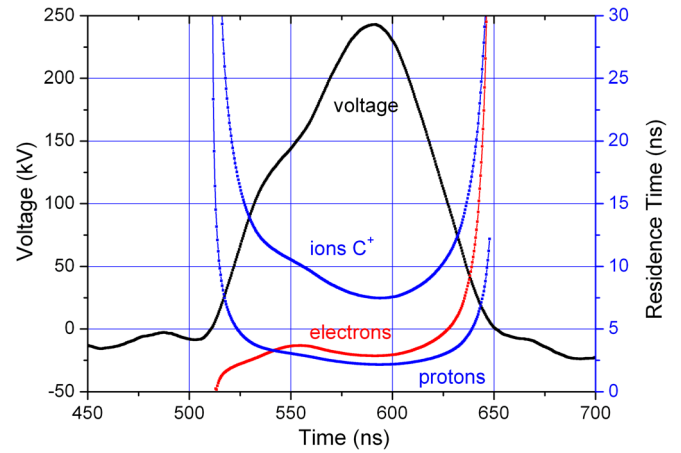


FIG. 11. (Color online) Oscilloscope trace of accelerating voltage and residence time of C^+ ions, protons, and electrons in the A-K gap.

$$\tau_{ion}(t) = \frac{v_{max}}{a} = \sqrt{\frac{2z \cdot U}{m_i}} \cdot \frac{d(t) \cdot m_i}{U(t) \cdot z} = \frac{[d_0 - v(t - t_0)]\sqrt{2m_i}}{\sqrt{z \cdot U(t)}},$$

where v_{max} is the ion velocity after passing through the A-K gap and a is the ion acceleration in the electric field.

Figure 11 shows the calculated electrons' drift time and the residence time of the ions in the A-K gap during the generation of an ion beam. The calculation was performed for the data in Fig. 3.

The calculation was performed for singly ionized carbon ions and protons, the average length of the electrons' drift was 11 cm and the A-K gap was 8 mm. Studies have shown that the electrons' drift time in the diode with magnetic self-insulation during the PIB generation is close to the protons' residence time in the A-K gap, and for C^+ ions, it is even less. This indicates the low efficiency of the magnetic insulation. The electron drift along the A-K gap of the diode with magnetic self-insulation does not provide suppression of the electron current. The increase in voltage on the potential electrode leads to an increase in the electron current in the diode, which consequently increases the magnetic induction because of the increase in current on the grounded electrode. The drift velocity changes insignificantly.

V. MECHANISM OF THE ELECTRON CURRENT SUPPRESSION

The analysis performed has shown that, under our experimental conditions in a diode with magnetic self-insulation and with an explosive potential electrode plasma forms effectively over the entire working area of the electrodes. But in spite of fulfillment of the conditions of magnetic insulation along the entire length of the diode ($B/B_{cr} \geq 4$) due to a high electron drift velocity, the time of their movement along the electrodes does not exceed the residence time of the ions in the A-K gap. In such circumstances, the total current of the diode should be equal to the estimated electron current whose current density is limited by the space charge. However, the experimental values of the total current during the PIB generation are less than those calculated (Eq. (1)) by a factor of 1.5–2 (see Fig. 3).

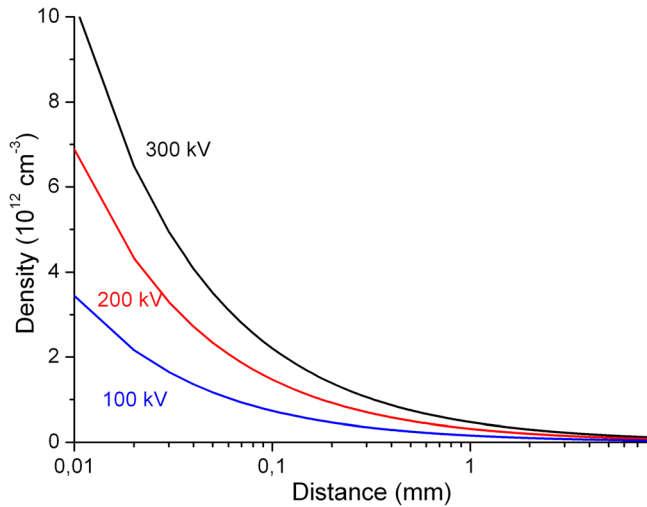


FIG. 12. (Color online) The distribution of the electrons in the space charge region.

The reduction in the electron current in the diode with magnetic insulation on the second pulse may be due to an increase in the density of the electrons at the surface of the grounded electrode (which is the cathode on the second pulse) due to the electrons drift. These electrons form a virtual cathode which prevents emission of the next coming electrons from the surface of the grounded electrode. The electron density distribution over the thickness of the space charge layer can be obtained from

$$j = \frac{4\epsilon_0}{9} \left(\frac{2e}{m}\right)^{1/2} \frac{U_0^{3/2}}{d^2} = e \cdot n_e(x) \cdot v_e(x),$$

where $n_e(x)$ is the concentration of electrons at a point with x coordinate and $v_e(x)$ is the velocity of electrons at this point.

Then, for $n_e(x)$,

$$n_e(x) = \frac{4\epsilon_0 U_0}{9e d^2} \left(\frac{d}{x}\right)^{2/3}.$$

Figure 12 shows the change in the concentration of electrons in the space charge region for different accelerating voltages.

The calculation was performed for an A-K gap of 8 mm. In our experimental conditions, the main part of the space charge region of the electrons which are emitted from the surface of the grounded electrode is concentrated in the area with a thickness of less than 0.1–0.3 mm. Calculations show that the electrons which have passed the space charge region then drift along the surface of the grounded electrode in a thin layer with a thickness of 0.4–0.5 mm (see Figure 9). They drift in the space charge of the electrons emitted from the surface of the grounded electrode. The average density of the electrons in the drift region is much higher than the electron density in the space charge region. This leads to an increase in the space charge density of the electrons, formation of the virtual cathode, interruption of the acceleration of the electrons from the plasma under the virtual cathode, and, as a consequence, a decrease in the

electron current density compared to that CL value calculated by Eq. (1).

This effect also leads to an increase in the ion current in the diode with magnetic self-insulation.⁹ Some of the electrons drift in the A-K gap in the ion space-charge region (near the surface of the potential electrode), providing an additional compensation of the ions charge and an increase in the ion current density by a factor of 5–9.

VI. CONCLUSION

Tests have shown that, in the diode with magnetic self-insulation in the double-pulse mode, there is an effective plasma formation on the entire surface of the explosive potential electrode. During the generation of the ion beam, the condition of magnetic cutoff of the electrons along the entire length of the diode is fulfilled ($B/B_{cr} \geq 4$). But, because of the high drift velocity, the electrons' drift time is close to the residence time of C^+ ions and protons in the A-K gap. This indicates that the efficiency of the magnetic insulation in the diode of the selected design is low. At the same time during the ion current generation, suppression of the electronic component by a factor of 1.5–2 is observed for the strip diode with both plane and focusing geometry. The reduction in the electron current in the diode with magnetic self-insulation on the second pulse may be due to an increase in the density of the electrons due to the electrons which drift at the grounded electrode surface. These electrons form a virtual cathode which prevents electron emission from the surface of the grounded electrode. The calculations show that the electrons which have passed the space charge region then drift along the surface of the grounded electrode in a thin layer with a thickness of 0.4–0.5 mm. The electron density in the drift region is 50–100 times higher than the density of the electrons in the space charge region. This leads to an increase in the electron space charge density, the formation of the virtual cathode, the suppression of the electrons' acceleration from the plasma under the virtual cathode, and, as a consequence, a decrease in the electron current density. The new mechanism provides a decrease in the electron current by limiting the emission of electrons from the explosive emission plasma rather than by increasing the time of their drift in the A-K gap.

ACKNOWLEDGMENTS

This work was supported by the Federal Target Program "Scientific manpower of innovative Russia" during the years 2009–2013, under Project No. P943.

¹I. Langmuir, *Phys. Rev.* **2**, 450 (1913); **33**, 954 (1929).

²R. N. Sudan and R. V. Lovelace, *Phys. Rev. Lett.* **31** (16), 1174 (1973).

³P. Dreike, C. Eichenberger, S. Humphries, and R. Sudan, *J. Appl. Phys.* **47**(1), 85 (1976).

⁴É. G. Furman, A. V. Stepanov, and N. Zh. Furman, *Tech. Phys.* **52**, 621 (2007).

⁵S. Humphries, *Plasma Phys.* **19**, 399 (1977).

⁶V. M. Bystrickii and A. N. Didenko, *High-Power Ion Beams* (Energoatomizdat, Moscow, 1984).

⁷X. P. Zhu, M. K. Lei, and T. C. Ma, *Rev. Sci. Instrum.* **73**, 1728 (2002).

⁸A. I. Pushkarev, J. I. Isakova, M. S. Saltimakov, and R. V. Sazonov, *Nature Sci.* **2**, 419 (2010).

- ⁹A. I. Pushkarev, Y. I. Isakova, and D. V. Vahrushev, *Phys. Plasmas* **17**, 123112 (2010).
- ¹⁰G. E. Remnev, I. F. Isakov, A. I. Pushkarev, M. S. Opekounov, V. M. Matvienko, V. A. Ryzhkov, V. K. Struts, I. I. Grushin, A. N. Zakoutayev, A. V. Potyomkin, V. A. Tarbokov, V. L. Kutuzov, and M. Yu. Ovsyannikov, *Surf. Coat. Technol.* **114**, 206 (1999).
- ¹¹P.L. Kalantarov and L. A. Tseydlin, *Calculation of the Inductances* (Energoatomizdat, Leningrad, 1986), p. 488.
- ¹²S. Humphries, *Charged Particle Beams* (Wiley, New York, 1990), p. 847.
- ¹³A. I. Pushkarev, J. I. Isakova, M. S. Saltimakov, and R. V. Sazonov, *Phys. Plasmas* **17**, 013104 (2010).
- ¹⁴A. I. Pushkarev and R. V. Sazonov, *IEEE Trans. Plasma Sci.* **37**(10), 1901 (2009).
- ¹⁵Z. Werner, J. Piekoszewski, and W. Szymczyk, *Vacuum* **63**, 701 (2001).
- ¹⁶H. A. Davis, R. R. Bartsch, J. C. Olson, D. J. Rej, and W. J. Wagenaar, *J. Appl. Phys.* **82**(7), 3223 (1997).